Study of Metal Oxide Catalysts by Temperature Programmed Desorption. 3. Formation and Reactivity of Adsorbed Oxygen over α-Ferric Oxide

Masakazu Iwamoto,** Yukihiro Yoda, Noboru Yamazoe, and Tetsuro Seiyama*

Department of Materials Science and Technology, Faculty of Engineering, Kyushu University, Hakozaki, Higashi-ku, Fukuoka 812

(Received November 17, 1977)

Formation and reactivity of oxygen adsorbates on the surface of α-Fe_2O_3 were investigated in the temperature range 0—600 °C by means of a temperature programmed desorption (TPD) technique. At least four different states of adsorbed oxygen were indicated by four TPD peaks, the maxima of which appeared at 50—300 (α), 350—360 (β), 480—490 (γ), and $>$600 °C (δ), respectively. Mode of preparation hardly affected the essential nature of oxygen adsorption (or desorption) except the relative amounts of respective desorptions. Of these adsorbates, α, whose desorption peak shifts over a wide temperature range depending upon adsorption conditions, was interpreted to be molecular oxygen (O_2 or O_2^-) bonded to the oxide surface with an extraordinarily broad heterogeneity, while β and γ species were tentatively assigned to O_2^- and O^-, respectively, adsorbed on different sites. The activation energies of desorption were 23.8 and 54.6 kcal/mol for β and γ, respectively. On exposure to gaseous hydrogen, β species as well as α turned more reactive than γ, though γ was also reactive at higher temperatures. The reaction of β and α species with hydrogen at lower temperatures gave rise to an increase in γ adsorption. This is accounted for by assuming a reaction in which the molecular adsorbates (α and β) react with hydrogen to leave the atomic adsorbates (γ) behind.

For an understanding of catalytic oxidation of reactants over metal oxide catalysts, it is important to know the kinds of oxygen adsorbates present on the oxide surface, their binding energies and populations, and how the structure or the preparation method of oxide catalysts affects the oxygen adsorption.

The problems might be best examined by use of a temperature programmed desorption (TPD) technique,[1] which adopts programmed heating of a catalyst surface covered with adsorbates. If all the adsorbates are in a given energy state, the increasing desorption probability with a rise in temperature results in a peak in the desorption flux; otherwise more than one peak are expected. The desorption temperature, peak shape and the variation of desorption temperature with the initial surface coverage are all related to the properties of adsorbates so that we can determine several adsorption (desorption) characteristics from the TPD chromatograms.[2] By this technique we studied oxygen adsorption on nickel oxide[3] and Cu(II) ion exchanged Y-type zeolite,[4] and revealed the existence of several modes of oxygen adsorbates on these adsorbents. We have applied the same technique to the investigation of oxygen adsorption on α-Fe_2O_3.

Ferric oxide, with the standard heat of formation ($-\Delta H_f^\circ$) of a moderate magnitude, exhibits high catalytic activity and selectivity for the oxidative dehydrogenation of butene to butadiene.[5] The correlation of the oxidation state of iron oxide with their catalytic activity has been discussed.[6,7] Fe_2O_3 is a n-type semiconductor in contrast to the p-type of NiO. It is of interest to compare the behavior of the two oxides. Recently, Halpern and Germain[8] examined the desorption of oxygen from powdered oxides of first transition metals by means of flash desorption. For Fe_2O_3 they obtained a spectrum with three desorption peaks at *ca.* 60, 250, and 550 °C. However, the limination of the method, *i.e.*, very rapid and non-linear heating (*ca.* 30 °C/s in average), prevented them from investigating the phenomenon in sufficient detail. The purpose of the present study is to clarify the formation, nature and reactivity of several modes of oxygen adsorbates on the surface of α-Fe_2O_3.

Experimental

Apparatus. The TPD apparatus is essentially the same as that used previously.[3] It consists of two parts; one in which sample conditioning and oxygen adsorption under specified conditions are carried out in the conventional manner, the other in which adsorbates on the sample undergo thermal desorption into a helium carrier under programmed heating. The concentration of the desorbed gas was monitored and recorded with a thermal conductivity detector.

Materials. Helium gas of ultra-high-purity grade ($>$ 99.995%) was supplied from Air Products and Chemicals. Before use, helium was passed through a liquid nitrogen cold trap in order to remove a trace amount of moisture. Oxygen gas was also dried before use by liquefaction and vaporization in a cold trap.

Ferric oxide samples were prepared by calcining ferric hydroxide, ferric nitrate or ferric oxalate, the corresponding sample being denoted by Fe_2O_3-I, II, or III, respectively. The calcination conditions and BET surface areas are summarized in Table 1. All the samples were identified to be α-Fe_2O_3 by X-ray powder diffraction. They were sieved to 20—60 mesh for TPD experiments.

Methods and Procedures. Ferric oxide, 1 g, was put into the TPD cell. Each fresh sample was evacuated for more than 2 h at 600 °C untill no more water was condensed in a liquid

Table 1. Ferric oxide samples

Catalyst	Starting materials	Calcination conditions	Surface area (m^2/g)
Fe_2O_3-I	$Fe(OH)_3$	600 °C, 5 h	5.5
Fe_2O_3-II	$Fe(NO_3)_3\cdot 9H_2O$	600 °C, 5 h	6.6
Fe_2O_3-III	$FeC_2O_4\cdot 2H_2O$	600 °C, 5 h	1.9

** Present Address: Department of Industrial Chemistry, Faculty of Engineering, Nagasaki University, Nagasaki 852.

nitrogen trap connected to the cell. The sample was then repeatedly subjected to a series of routine TPD procedures consisting of sample pretreatment, oxygen adsorption and temperature programmed desorption. As pretreatment, the sample was exposed to 100 Torr of oxygen for 1 h followed by evacuation ($<10^{-5}$ Torr) at 600 °C for 1 h. Oxygen was usually adsorbed according to one of the following ways.

Procedure I: After being cooled to the desired temperature, the sample was exposed to an oxygen atmosphere (100 Torr) for 1 h and then evacuated for 15 min before further cooling down to 10 °C within 30 min *in vacuo*.

Procedure II: On the introduction of 100 Torr of oxygen at 600 °C, the sample was made to cool at a rate of *ca.* 10 °C/min down to 10 °C, at which the system was evacuated for 15 min.

After these manipulations, a carrier gas (helium) was diverted to flow through the reactor at a rate of 30 cm^3/min and the programmed heating was started. The heating rate was 21 ± 1 °C/min unless specified otherwise. The thermally desorbed oxygen was recorded as a TPD chromatogram, its amount being evaluated from the peak area of the chromatogram.

In order to examine the reactivity of adsorbed oxygen toward hydrogen, various amounts of hydrogen were injected in a pulse at specified temperatures, with a helium carrier (30 cm^3/min). After ten min from the hydrogen pulse, the sample was cooled to 10 °C and heated up to take a TPD chromatogram. In all these runs, a liquid nitrogen trap was equipped between the TPD cell and the detector in order to separate off water vapor desorbed from the reacted surface. The monitored gas was identified to be oxygen alone throughout the experiments by gas chromatography and mass spectroscopy.

Results and Discussion

Desorption Chromatograms of Oxygen from Fe_2O_3. Desorption chromatograms of oxygen from Fe_2O_3 were found to vary with the sample preparation and conditions of oxygen adsorption. Figures 1 and 2 show typical examples obtained for Fe_2O_3-I and II, respectively, after oxygen adsorption was performed at various temperatures by Procedure I (all runs except 1 and 6) or II (runs 1 and 6) as indicated. Although the amounts of oxygen desorption are dependent upon sample preparation to some extent, oxygen desorption is reproducible in the same temperature range irrespective of the sample preparation if oxygen has been adsorbed under the same conditions. The change in adsorption temperature T_{ad}, however, cause pronounced effects on TPD chromatograms, since it affects the states and concentrations of adsorbed oxygen. Thus, for various T_{ad} values five desorption peaks appear whose maxima appear respectively at 50—70 (α_{10}), 180—200 (α_{110}), 350—380 (β), 480—490 (γ), and >600 °C (δ). The subscripts attached to α for the first two peaks denote T_{ad}. The peaks are assigned to the same kind of oxygen species adsorbed on a heterogeneous surface. The desorption peak δ appears invariably in all the chromatograms with similar shapes and magnitudes, suggesting that it is a sort of desorption of lattice oxygen from Fe_2O_3 toward a non-stoichiometric oxide. In contrast, the other peaks change in magnitude markedly with the conditions of oxygen adsorption and can be attributed to adsorbed oxygen species. β and γ peaks, which also appear in chromatograms 1 and 6, can be assigned to respective kinds of oxygen adsorbates. On the other hand, a marked feature of the α species is the desorption temperature shifts over a wide range from room temperature to *ca.* 300 °C, depending on T_{ad}.

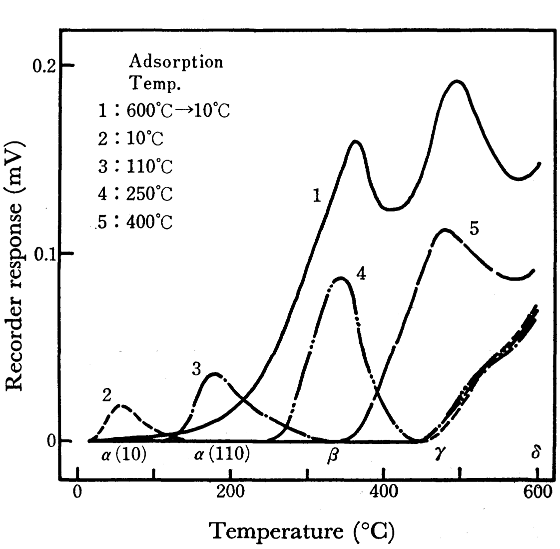

Fig. 1. TPD chromatograms of oxygen adsorbed on Fe_2O_3-I.

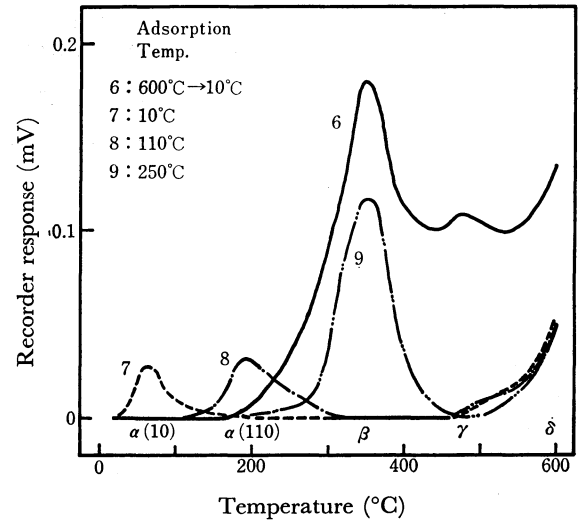

Fig. 2. TPD chromatograms of oxygen adsorbed on Fe_2O_3-II.

The amounts of desorbed (or adsorbed) oxygen per unit surface area (V_d) were determined from the

Table 2. Amounts of desorbed oxygen from the ferric oxides

Adsorption temp (°C)	Desorption peak	Amount of desorbed oxygen (cm^3/m^2)		
		Fe_2O_3-I	Fe_2O_3-II	Fe_2O_3-III
10	$\alpha(10)$	1.88×10^{-4}	2.19×10^{-4}	4.86×10^{-4}
110	$\alpha(110)$	4.34×10^{-4}	3.00×10^{-4}	3.96×10^{-4}
250	β	9.22×10^{-4}	1.07×10^{-3}	1.80×10^{-3}
400	γ	1.73×10^{-3}		3.81×10^{-3}
600→10	$\beta+\gamma+\delta$ a)	4.39×10^{-3}	3.15×10^{-3}	1.18×10^{-2}

a) Total oxygen desorbed below 600 °C.

desorption peak areas, data for the three samples being summarized in Table 2. For runs in which Procedure II was used for oxygen adsorption, only the total amounts of oxygen desorbed below 600 °C ($\beta+\gamma+\delta$) are given. The amounts are in the order $\alpha_{10} \lesssim \alpha_{110} < \beta < \gamma$, differing somewhat with sample. We can estimate the surface coverage from these values. The amount of $\beta+\gamma+\delta$, for example, is 4.39×10^{-3} cm^3/m^2 or 1.18×10^{13} oxygen molecules/cm^2 for Fe_2O_3-I. If we assume that the adsorbent surface is (0001) or $(11\bar{2}0)$ plane of α-Fe_2O_3 which contains 4.55×10^{14} or 2.92×10^{14} surface iron atoms/cm^2, respectively, the above value corresponds to only *ca.* 0.02 or 0.04 O_2 molecules per surface iron atom, respectively. This suggests that some sort of surface defect is responsible for the oxygen adsorption. There is little possibility that oxygen adsorbs on a surface impurity, since the desorption of oxygen is inherent for each oxide and the amount of desorbed oxygen seems to be related with the heat of oxide formation ($-\Delta H_f^\circ$).[9]

It is interesting to compare the adsorptive properties of Fe_2O_3 (a n-type semiconductor) and NiO (a p-type semiconductor). The TPD experiments show that the surface coverage of adsorbed oxygen is nearly the same for both oxides. This suggests that, contrary to the accepted view, the type of semiconductor has little effect on the amount of adsorbed oxygen.

Sample preparation affects only the relative amounts of desorption peaks, the essential nature of the oxygen desorption (or adsorption) remaining unaffected. Thus the experiments were performed only with Fe_2O_3-I. Interconversion between the oxygen adsorbates is negligible during the course of evacuation, cooling, and heating applied. For instance, chromatogram 4 which shows a single desorption peak, β, indicates that none of β adsorbates were converted into γ, α_{110}, or α_{10} during the TPD experiments. Similar conclusions can be drawn from the other runs.

Characterization of Desorption Peaks. Oxygen desorption below 350 °C was investigated in detail. Figure 3 shows the effect of oxygen adsorption temperature (T_{da}) on the TPD chromatogram. In each case of $T_{ad}=10$, 110, and 160 °C, a single desorption peak appears below 400 °C; oxygen desorption starts at a temperature near T_{ad}, reaches a maximum around a temperature 40—80 °C higher than T_{ad} and then decreases with a very long tailing. With $T_{ad}=200$ °C, however, there appear two desorption peaks with maxima at 280 and 350 °C, the former apparently being of the same feature as the above and the latter assignable to β desorption. Further increase in T_{ad} to 250 °C again gives rise to a single desorption peak (β) at 350 °C. This indicates that the desorption peak at the lower temperature region shifts continuously with T_{ad}. Such a phenomenon can not be explained in terms of the change in the kind of adsorbed species, but is best understood in terms of a single kind of adsorbate (α) desorbing from the oxide surface with a broad heterogeneity, though the actual nature of the adsorption sites is not clear. It is assumed that, while α adsorbates can take continuous adsorption states with broadly dispersing bonding energies, at a given T_{ad} only α species with a certain range of bonding energies are formed. In connection with such behavior of α desorption, it is noted that remarkable leadings are seen, prior to the β peak (Figs. 1 and 2, runs 1 and 6). These are considered to be partly contributed by the broadly dispersed α desorption. The β peak maxima (350—360 °C) are scarcely affected at all by adsorption conditions, showing little heterogeneity associated with it.

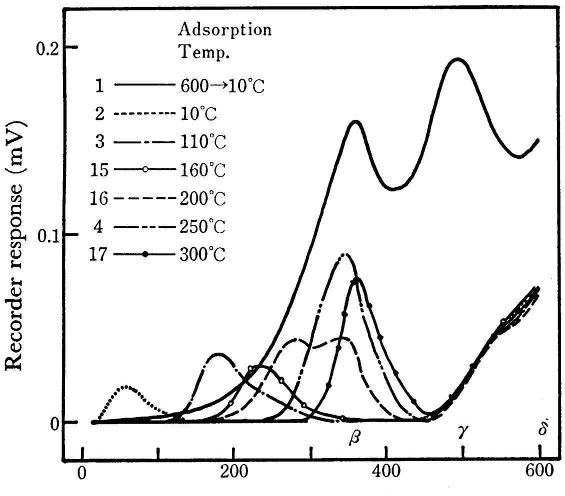

Fig. 3. Effect of the adsorption temperature on TPD chromatograms of oxygen.

Interactions between oxygen adsorbates were studied as follows.

(1) The sample on which oxygen had been adsorbed at 110 °C was further exposed to an oxygen atmosphere (100 Torr) at 10 °C for 1 h. The results coincided with these in chromatogram 3, indicating that the presence of α_{110} inhibits adsorption in α_{10}. Probably the oxide surface had been saturated with α_{110}, no more room being left for α_{10}.

(2) After β species was adsorbed in the same way as for chromatogram 4, the sample was further exposed to 100 Torr of oxygen at 110 °C for 1 h. The chromatogram obtained showed two desorption peaks of α_{110} and β. The amount of α_{110}, 2.1×10^{-4} cm^3/m^2, was about a half of that for chromatogram 3, whereas that of β, 9.1×10^{-4} cm^3/m^2, was almost the same as for chromatogram 4. Suppression of α_{110} as compared with chromatogram 3 suggests a steric or electrostatic hindrance by β species.

(3) A sample, exposed to 100 Torr of oxygen at 600 °C for 1 h in advance, was cooled down to 10 °C at a rate of *ca.* 10 °C/min in the same atmosphere, with pause at 400 °C for 1 h. The resulting chromatogram was in precise agreement with chromatogram 1. This shows that all the adsorption sites for β and γ are fully occupied in chromatogram 1 (Procedure II), and that β and γ do not interact with each other, or in other words, they adsorb on independent adsorption sites.

For β and γ species, the activation energies of desorption were measured on the basis of the equations derived by Cvetanovic and Amenomiya.[1] When the sample temperature increases linearly with time at a heating rate b and desorption takes place from a homogeneous surface without appreciable readsorption, we obtain Eqs. 1 and 2, for the first order and second order desorptions, respectively.[2,10,11]

$$2\ln T_{\mathrm{M}} - \ln b = \frac{E_{\mathrm{d}}}{RT_{\mathrm{M}}} + \ln\frac{E_{\mathrm{d}}v_{\mathrm{m}}}{Rk_0} \qquad (1)$$

$$2\ln T_{\mathrm{M}} - \ln b = \frac{E_{\mathrm{d}}}{RT_{\mathrm{M}}} + \ln\frac{E_{\mathrm{d}}v_{\mathrm{m}}^2}{2Rk_0} - \ln v_{\mathrm{m}}\theta_{\mathrm{M}} \qquad (2)$$

Here T_{M} is the temperature of the desorption peak maximum, v_{m} the amount of adsorbate at the full surface coverage, θ_{M} the surface coverage at the peak maximum, and k_0 and R are constants. In the first order desorption, when T_{M} is measured as a function of b, E_{d} can be obtained from the plots of ($2\ln T_{\mathrm{M}}-\ln b$) *vs.* $1/T_{\mathrm{M}}$. For the second order desorption, the computer simulation analyses of TPD chromatograms[12] show that θ_{M} is little affected by b if the initial surface coverage is kept constant. Based on Eq. 2, the conditions allow us to evaluate E_{d} of the second order desorption also from the same plots as above. This means that we can estimate E_{d}, at least as an approximation, from the same plots without knowing exact desorption orders. Recently Konvalinka *et al.* reached the same conclusion by computer simulation analyses.[13] Such an approximation is permissible only for the homogeneous surface.[14]

TABLE 3. TEMPERATURE PROGRAMMED DESORPTION OF β AND γ OXYGEN

β oxygen			γ oxygen		
b °C/min	T_{M} K	V_{d} cm^3/m^2	b °C/min	T_{M} K	V_{d} cm^3/m^2
10.0	609	2.44×10^{-3}	9.1	745	1.27×10^{-3}
			9.5	745	1.31
15.0	616	2.46	14.5	755	1.34
20.0	624	2.48	18.5	759	1.24
25.0	632	2.46	22.3	761	1.16
30.0	641	2.42	29.0	766	1.42

b heating rate, T_{M} peak temperature, and V_{d} desorbed amount.

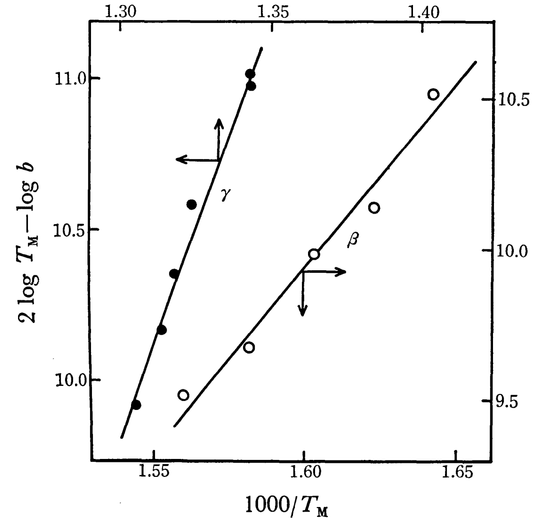

Fig. 4. Activation energy of desorption for β and γ adsorbates.

The analyses were applied to β and γ desorption. In order to obtain respective desorption peaks in adequate magnitudes, oxygen adsorption was performed by Procedure II for β, and by Procedure I for γ at 410 °C. In the analyses of β, the contribution of α adsorbates to the leading part was disregarded. The results are summarized in Table 3. For both cases of β and γ, T_{M} increases with increase in b. The plot of ($2\ln T_{\mathrm{M}}-\ln b$) *vs.* $1/T_{\mathrm{M}}$ gave straight lines in agreement with the above equations (Fig. 4). From the slopes, the activation energies for β and γ were determined to be $E_{\mathrm{d}}(\beta)=23.8$ and $E_{\mathrm{d}}(\gamma)=54.6$ kcal/mol, respectively.

The desorption orders for β and γ remain undetermined. Phenomenologically, differentiation of the desorption order can be made according to whether or not T_{M} is independent of the amount of adsorbates (V_{d}) at a constant heating rate. No experiments were carried out for the sake of confirmation. However, there is some evidence that β and γ desorption are of the first and second order, respectively. Figure 3 shows that T_{M} of β desorption is almost unchanged with a change in magnitude of the desorption peak (runs 1, 4, 16, and 17), suggesting the first order desorption. On the other hand, T_{M} of γ desorption shifts to the higher side with a decrease in V_{d} (Figs. 6 and 7), indicating the second order desorption.

Winter[15] has studied the isotopic exchange reaction of oxygen over α-$\mathrm{Fe_2O_3}$ pretreated in various ways, and found that the activation energy of the reaction is 19—27 kcal/mol at 260—400 °C. The value is in good agreement with $E_{\mathrm{d}}(\beta)$. It appears that the rate determining step of the reaction is the desorption of molecular oxygen from the surface, in line with Winter's suggestion.

Reaction of Adsorbed Oxygen with Hydrogen. The oxygen adsorbates were found to react easily with hydrogen. After oxygen adsorption by Procedure II, the sample was brought in contact with a hydrogen pulse (0.025—0.200 cm^3 (STP)) at selected temperature.

The effect of the pulse (reaction) temperature on the TPD chromatogram is shown in Fig. 5. The hydrogen pulse, 0.05 cm^3, is twice the amount necessary to convert all the adsorbed oxygen into $\mathrm{H_2O}$. The left part of the peak β disappears at 80 °C or below. α adsorbates are consumed simultaneously under these conditions, since this part is partly contributed by the α desorption as mentioned above. With an increase in temperature up to 188 °C, increasing amounts of β are consumed. Such consumption of β adsorbates (and α in part) is coupled with a roughly proportional increase in γ desorption. Thus the γ desorption becomes the largest after the hydrogen pulse at 188 °C. It was cinfirmed that the γ species also reacts with hydrogen above 300 °C.

The effect of the amount of hydrogen pulse at 125 °C on TPD chromatogram is shown in Fig. 6. Increase in pulse amount up to 0.2 cm^3 causes γ desorption to increase at the expense of β (and α), in a similar manner to that above. Since the injection of 1.0 cm^3 of hydrogen gave a chromatogram almost the same as chromatogram 30, it is concluded that γ adsorbates are inactive to hydrogen at 125 °C. Whilst all the adsorbates are able to react with hydrogen under adequate conditions, α and β adsorbates are much more reactive than γ.

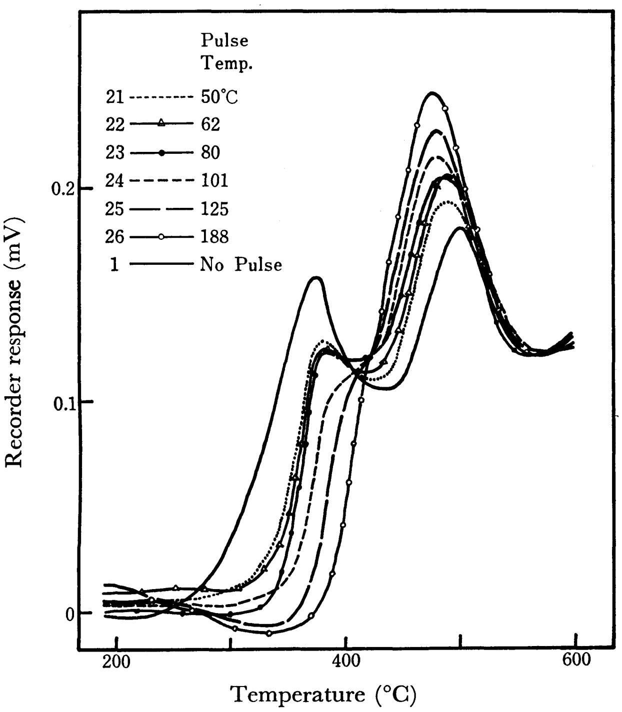

Fig. 5. TPD chromatograms of oxygen adsorbed on Fe_2O_3-I after the reaction with hydrogen pulsed at various temperature.

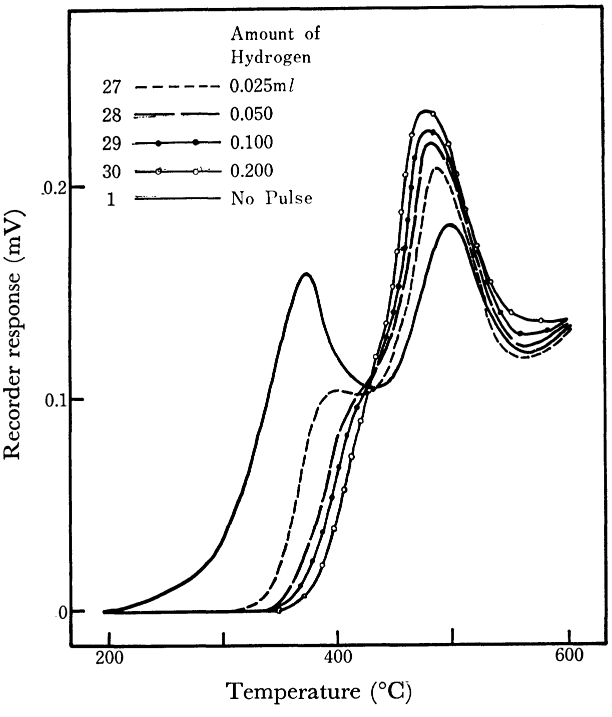

Fig. 6. Influence of the pulse amounts of hydrogen on TPD chromatograms of oxygen adsorbed on Fe_2O_3-I.

Table 4. Reaction of oxygen adsorbed on Fe_2O_3-I with hydrogen

Run No.	Reaction temp (°C)	Amount of hydrogen pulse (cm^3)	Decrease in β, V_{dec} (cm^3/m^2)	Increase in γ V_{inc} (cm^3/m^2)	$\frac{V_{inc}}{V_{dec}}$
21	50	0.05	0.65×10^{-3}	0.22×10^{-3}	0.34
22	62	0.05	0.70	0.38	0.54
23	80	0.05	0.95	0.44	0.46
24	101	0.05	1.10	0.59	0.53
25	125	0.05	1.52	0.69	0.45
26	188	0.05	1.79	0.91	0.51
27	125	0.025	1.31	0.53	0.40
28	125	0.050	1.52	0.69	0.45
29	125	0.100	1.77	0.95	0.54
30	125	0.200	1.79	1.14	0.64

Why does the γ adsorbates increase coupled with the consumption of β (and α)? For each run in Figs. 5 and 6, the amounts of decrease in $\beta(V_{dec})$ and increase in $\gamma(V_{inc})$ were determined from the respective peak areas. It was found that the relation $V_{inc}/V_{dec}\simeq1/2$ holds in all runs (Table 4). To account for this relation, we assume that α and β adsorbates are molecular while γ is atomic, and that the molecular species reacts with hydrogen at 50—188 °C to leave the atomic species (γ) behind. The reaction may be represented as follows, if the electronic states of adsorbates are disregarded.

$$O_2(ad) + H_2 \longrightarrow O(ad) + H_2O$$

Since adsorption in γ must have been saturated after the oxygen adsorption by Procedure II, the increase of adsorbates indicates that additional sites for γ adsorption are created by the above reaction. It was confirmed that oxygen adsorption by Procedure II after the pulse reaction gave precisely the same TPD chromatogram as in run 1. This indicates that the surface can be brought back reversibly to the original state during the course of adsorption. It seems that the hydrogen pulse creates additional γ sites to accommodate atomic oxygens. It is possible that β sites are made to turn into γ sites tempolarily due to the chemical reaction involved.

The assumption that α and β adsorbates are molecular is not unreasonable, considering that they form or desorb at relatively low temperatures. β desorption shows a feature of the first order desorption in which the desorption temperature is little affected by the surface coverage. In contrast, the desorption temperature for γ is dependent on the surface coverage as exemplified by chromatograms in Figs. 5 and 6, a feature of the second order desorption or the dissociative adsorption. The plots of log V_{dec} *vs.* inverse of the pulse temperature give a straight line. From the slope, the activation energy for the above reaction was obtained as 4.5 kcal/mol, which may correspond to the energy of rupturing O–O bond in the molecular adsorbates.

There is no definite evidence to indicate the electronic states of α, β, and γ adsorbates. However, many metal oxides have been known to adsorb oxygen as O_2 or O_2^- at relatively low temperatures, while adsorption as O^- or O^{2-} is favored at higher temperatures. At present, we assume tentatively that α, β, and γ adsorbates are O_2 or O_2^-, O_2^-, and O^-, respectively.

The reactivity of adsorbed oxygen exhibits very interesting features not so far foreseen, though the assumption used to interpret them needs further verification. This kind of information would be important for the understanding of catalytic oxidations.

References

1) R. J. Cvetanović and Y. Amenomiya, *Adv. Catal.*, **17**, 103 (1967).

2) M. Smutek, S. Cerny, and F. Buzek, *Adv. Catal.*, **25**, 343 (1975).

3) M. Iwamoto, Y. Yoda, M. Egashira, and T. Seiyama, *J. Phys. Chem.*, **80**, 1989 (1976).

4) M. Iwamoto, K. Maruyama, N. Yamazoe, and T. Seiyama, *J. Phys. Chem.*, **81**, 622 (1977).

5) G. C. A. Shuit, *ACS Adv. Chem. Ser.*, **76**, 261 (1968).

6) G. K. Boreskov, V. V. Popovskii, and V. A. Sazonov, *Proc. 4th Intern. Congr. Catalysis, Moscow*, 1968, Vol. 1, p. 439.

7) M. Misono, Y. Nozawa, and Y. Yoneda, *Proc. 6th Intern. Congr. Catalysis, London*, 1976, Vol. 1. p. 386.

8) B. Halpern and J. E. Germain, *J. Catal.*, **37**, 44 (1975),

9) M. Iwamoto, Y. Yoda, N. Yamazoe, and T. Seiyama, *J. Phys. Chem.*, in press.

10) Y. Amenomiya and R. J. Cvetanović, *J. Phys. Chem.*, **67**, 144, 2046, 2705 (1963).

11) J. L. Stakebake, *J. Phys. Chem.*, **77**, 581 (1973).

12) M. Iwamoto and T. Seiyama, unpublished results.

13) J. A. Konvalinka, J. J. F. Sholten, and J. C. Rasser, *J. Catal.*, **48**, 365 (1977).

14) The method of determining E_d over the heterogeneous surface has been investigated: Y. Tokoro, M. Misono, T. Uchijima, and Y. Yoneda, *Bull. Chem. Soc. Jpn.*, **51**, 85 (1978).

15) E. R. S. Winter, *J. Chem. Soc.*, *A*, **1968**, 2889.